Int. J. Nano Dimens., 9 (2): 134-144, Spring 2018

ORIGINAL ARTICLE

First principle study of structural and electronic transport properties for electrically doped zigzag single wall GaAs nanotubes

Debarati Dey[1, 2 *], *Debashis De*[1, 3]

[1] *Deptartment of Computer Science and Engineering Maulana Abul Kalam Azad University of Technology, BF-142, Sector 1, Salt Lake City, Kolkata – 700 064, West Bengal, India*

[2] *Deptartment of Electronics and Communication Engineering B. P. Poddar Institute of Management and Technology, 137, V. I. P Road, Kolkata – 700 052, West Bengal, India*

[3] *Department of Physics, University of Western Australia, M013, 35 Stirling Highway, Crawley, Perth, WA 6009, Australia*

Received 29 September 2017; revised 27 December 2017; accepted 07 January 2018; available online 10 January 2018

Abstract

Emerging trend in semiconductor nanotechnology motivates to design various crystalline nanotubes. The structural and electronic transport properties of single walled zigzag Gallium Arsenide nanotubes have been investigated using Density Functional Theory (DFT) and Non-Equilibrium Green's Function (NEGF) based First Principle formalisms. Structural stability and enhanced electronic transmission property of Gallium Arsenide nanotubes (NT's) have been analyzed for the chiral vector $3 \leq n \leq 7$**.** This analysis based on the Perdew Burke Ernzerhoff type of parameterization along with Generalized Gradient Approximation (GGA) procedure. Several structural properties like dependency of diameter along with bond length, buckling and band gap have been analyzed. The investigation confirms that buckling property and bond length of these nanotubes decreases as the diameter of the tubes are increasing. It has been observed that (7, 0) nanotube is being considered as most stable nanotube among all. Binding energy also increases with the increasing diameter of the tubes. This two probe experiment is being carried out at room temperature when two opposite bias voltages have given at the end of these nanotubes using electrical doping procedure. Introducing this procedure a potential drop has been created between the two electrodes' chemical potential level. Due to this potential drop, the device performance has been enhanced and results in the flow of high conducting current through the central part of the NTs'.

Keywords: *Chiral Vector; DFT; GaAs; Nanotube; NEGF.*

How to cite this article

Dey D. First principle study of structural and electronic transport properties for electrically doped zigzag single wall GaAs nanotubes. Int. J. Nano Dimens., 2018; 9 (2): 134-144.

INTRODUCTION

Gallium Arsenide (GaAs) is one of the most challenging and direct band gap semiconductor, which plays an important role in semiconductor nanotechnology. Due to the direct band gap property, GaAs plays the crucial role in the optical domain. Since the evolution of Carbon Nano Tube (CNT), tremendous theoretical and experimental research works have been demonstrated all over the world. Quantum transport properties, spin-filtration property and spin transport of CNT have been investigated when CNT formed composites with Copper, Chromium, and Iron [1-3]. CNT has also been proved as high sensing device when it senses NO_2 molecules or any foreign molecules [4-6]. Researchers have also investigated several types of nanotubes (NTs) and their quantum-mechanical properties [7-14]. Several properties like structural and quantum-transport phenomenon, voltage and spin dependent transportation features, effect of moister and defect and absorption effects have been demonstrated for these NTs using Density Functional Theory (DFT) and Non-Equilibrium Green's Function (NEGF) based First Principle approach.

In this paper, the structural stability and quantum-ballistic properties of electrically doped GaAs NTs have been investigated at room

* Corresponding Author Email: *debaratidey@yahoo.com*

temperature (300 K). By introducing electrical doping procedure, the potential drop has been generated along the electrodes of the NT. Electrical doping is the procedure of introducing of electronic charge donation or electronic charge acceptation to the nanoscale devices. The importance of this process is that the conventional doping process can be avoided which generates different types of defects into the nanoscale device design process. In 1998, this doping process has been introduced for the molecular films. Furthermore, this process has been successfully demonstrated for n-type III-V inorganic compounds [15, 16].

In optical domain, for the design of Organic Photo Voltaic Cell (OPVC), this process has also been used to tune the energy level alignment [17]. Enhanced device efficiency, carrier injection can be achieved using electrical doping process for both n and p-type dopants to a large extent [15, 18]. Henceforth, it has been realized that electrical doping process has several advantages over conventional doping process. Optimization of n-type III-V Nitrides results in enhanced contact resistance, biasing voltage, carrier insertion and recombination [16, 19-21]. By introducing this doping process several nanoscale devices like the diode, FET can be designed and characterized [19-21]. The proposed GaAs NT has been compared with some of the NTs in Table 1.

In this paper, a single walled zigzag GaAs nanotube has been designed with various chiralities. The diameter of the nanotubes varied according to the chiralities. The diameter dependent band gap, buckling, binding energy (E_b), I-V response, device density of states (DDOS) and transport properties have been discussed. This paper presents the structural stability of GaAs NTs for several chiralities ($3 \leq n \leq 7$).

The main aim of this paper is to investigate the change of electronic quantum-ballistic transmission properties when the number of chiral vector increases from 3 to 7. Generally, chiral vector signifies the type of NTs that means whether the NTs obtained the nature of semiconductor or metallic. The Chiral vector can be represented as (n, m). These values also signify whether the form of the tube is zigzag or armchair. If m=0, then the tube is zigzag and if n=m then the tube looks like the armchair. If n-m= 3i, if i is the integer, then the NT is metallic, if i is non-integer, then the NT is the semiconductor. Therefore, in this paper, we have concentrated to investigate the change in the quantum-ballistic electronic transmission nature when the value of n increases from 3 to 7. It has also been investigated to check the structural stability of the tubes when increases the chiralities.

The paper illustrates the various structural and quantum-ballistic electronic transmission properties:

- Investigate the diameter dependence of the structural and electronic properties.
- Buckling decreases with the increasing chiralities.
- Current conductivity increases as the chiralities increase.
- Binding energy increases with the increasing diameter of the tube. I_{ON}/I_{OFF} ratio increases for the high chiral vector.

Table1: Novelty of the proposed GaAs NT using first principle approach compared with existing NTs.

Features \ ExistingNTs	ZnO NT [22]	SiC NT [11]	GaN NT [13]	SiNT [10]	CNT [6]	Proposed GaAs NT
Based on	DFT+NEGF	DFT+NEGF	DFT+NEGF	First Principle	DFT+NEGF	DFT+NEGF
Applied Bias Voltage (V)	±4	-2-+2	-4-+4	-	+1	±1.5
Maximum Diameter of NT (nm)	20-100	-	0.92	-	0.784	0.921
Operating Frequency	-	-	-	-	-	1000THz
Stress Tolerance (eV/Å^3)	-	-	-	-	-	0.01
Force Tolerance(eV/Å)	0.005	0.05	0.05	0.05	-	0.001
Optical range	-	-	-	-	-	Mid-UV
Chiral vector	(8, 0)	-	(4, 0)	-	-	(n, 0), 3≤n≤7
Maximum Current (μA)	115 (approx)	0.25	139	-	-	139.8
Switching Property	-	-	Satisfactory	-	-	Good
Electron Temperature	-	1000K	300K	-	0-200°C	300K
Doping	No doping	No doping	No doping	No doping	No doping	Electrically doped

EXPERIMENTAL

The analytical model of zigzag single wall GaAs NT has been presented using DFT and NEGF based first principle approach. This semi-empirical model of this NT has been investigated and illustrated using Atomistix Tool Kit- Virtual Nano Laboratory (ATK-VNL) software package version 13.8.0 [23-25]. The various simulation parameters have been chosen according to the chiral vectors. The pre-optimized single walled GaAs NT has been designed for chiralities (n, 0) where $3 \leq n \leq 7$. MONO hybridization procedure has been chosen for the central atomic part of the NT device. The device is therefore geometrically optimized by minimizing atomic level force and stress. The quantum-ballistic transmission has been carried out using Keldysh NEGF and DFT formalism. The atomic scale device is divided into three parts viz: left electrode, right electrode, and central atomic region. The two probe experiment has been implemented using single zeta polarization method. Table 2 presents the detail list of the simulation parameters and their values.

The various nanoscale electronic structures can be analytically designed and calculated using DFT. The first principle quantum mechanical property along with quantum transport phenomenon can be described using DFT. In the year of 1964 and 1965, Hohenberg-Kohn and Kohn-Sham introduced this theory [23-24]. The molecular level multi electronic nanoscale system can be designed theoretically using this formalism. This theory is highly desirable for computational physics, computational chemistry, nano-bio molecular design, spintronics, quantum-mechanical analytical design etc. Various analytical calculations can be done using DFT.

- Design of nanoscale electronic structure with electronic doping [26].
- Energy classification for atomic scale materials, which is applicable both for solid and fluid [26].
- This theory provides analytical analysis for the

Table 2: Simulation parameters.

Parameter	Value
Configuration	(x, y, z)
Fermi level	0 eV
Optical range	Mid-UV (UV-B)
Wavelength	300nm
Atomic Force	0.001eV/Å
Atomic Stress	0.01eV/Å^3
Poisson Solver	FFT2D
Input voltage	0V-±0.02V
Mesh cut-off density	10Ry
Basis sets	Hoffmann
Device algorithm	Krylov
Close neighbour distance	0.01nm
Maximum nos. of steps	200
Step size	0.02nm
K-points	1×1×100
Generic wighting Scheme	Wolfsberg
Exchange correlation function	Local Density Approximation-Generalized Gradient Approximation (LDA-GGA)
Basis set	Single Zeta Polarization
Hybridization	MONO
Hückel Basis set	Hoffmann
Time period	1fs

atomic level materials [26].
- Various features of matters can be calculated like; transmission spectrum, Device Density of States (DDOS), Local Device Density of States (LDDOS), Chemical potential. Complex Band structure, etc [26].
- This theory also helps to investigate the effectiveness of spin polarization models [26].

British mathematician George Green developed non-equality of atomic scale matter in the year of 1830. This concept has been used for molecular scale device designing. This function has been used to calculate two space time coordinates. This theory is associated with perturbation theory which calculates the various properties of matters like electronic interaction, atomic perturbation, momentum, current density, electron energies etc [26]. NEGF formalisms have been used to characterize the quantum mechanical structures of nanoscale devices [27- 29].

In this paper, electrical doping has been employed at the two ends of the extended part of the GaAs NTs. This doping helps to create a voltage drop across the central region and generates carrier transmission from one end to another of the NTs. In this case, we have applied equal but opposite polarity bias voltages at the two ends of the NTs. Therefore the two sides of the device can be acted as p and n-type. This potential drop enhances the device performance by increasing the channel conductivity. Thus it can be assumed that the p region has been considered as source and n region has been considered a drain. So that conventional current flows from source to drain region. The channel conductivity highly depends on the availability of the energy states around energy level E, which is equivalent to the electrode's chemical potential μ *i.e.* E=μ. These energy states may be filled or vacant that does not affect the channel conductivity. When the energy level lowers at the drain region compared with source due to applied voltages, then electron starts to flow. This phenomenon can be explained in Eq. (1).

$$qV_d = \mu_1 - \mu_2 \quad (1)$$

In Eq. (1), q is the columbic charge, V_d is the voltage difference between source and drain, μ_1 and μ_2 are the chemical potentials of left and right electrodes, respectively. In this case as the electrodes' material remains same GaAs, so these values are same at a particular bias voltage. Thus to create voltage drops the potentials of two electrodes are kept at same bias voltage but with opposite polarity. Source region tries to pump electrons into the central region where a drain region pulls out the electron and therefore equilibrium never been reached. So the electronic transmission remains continue. This electronic doping is different from conventional doping because no such foreign molecules have been incorporated in this case. This electrical doping procedure helps to create potential drop across the device. In this paper, the structural stability and electronic transport properties have been investigated by increasing the chiralities of GaAs NTs. The various zigzag GaAs NTs are shown in Fig. 1(a) to (e) for different chiralities.

RESULTS AND DISCUSSIONS

This nanoscale GaAs NTs' have been designed using DFT and NEGF based first principle formalisms. These analytical models of NTs have been illustrated theoretically at room temperature. The operating frequency has been kept at 1000THz, thus this NT can be used further as ultra high speed device. In this paper, the chiral vector (n, 0) has been taken from $3 \leq n \leq 7$. It has been proved that higher the device diameter higher is the stability. This also improves the quantum-ballistic transport property of the device.

The theoretical model of GaAs NT has been divided into three regions; the left electrode, right electrode along with scattering region. The left and right electrodes have some extension at the molecular level. This device has been simulated using Atomistix Tool Kit- Virtual Nano Laboratory (ATK-VNL), Quantum wise software simulation package version. 13.8.0. Transmission spectra T(E) at the molecular level is highly energy dependent. This electronic transmission obeys the quantum-mechanical transport phenomenon. The electronic transmission happens due to the potential drop between the two electrodes, which is generated due to the electrical doping procedure. Though this transmission is partially either exaggerated or diminished due to the quantum-ballistic backscattering effect. Transmission T(E) can be expressed as in Eq. (2), where T(E) depends on Device Density of States (DDOS), energy level E, self-consistent potential U and broadening effect γ [30].

$$T(E) = D(E - U)2\pi\gamma_1\gamma_2\gamma \quad (2)$$

This broadening effect for two electrodes represented as γ_1 and γ_2. Thus it can be observed from the Eq. (2), that better quantum-ballistic transmission depends on the larger number of available energy states and broadening of the peaks of DDOS. The comparative transmission spectra are shown in Fig. 2. However, it can be seen from Fig. 2, that maximum broadening effect with a large number of available energy states can be observed for (7, 0) NT. So it can be considered that higher the chiralities, higher will be the transmission. From this, we also can state that electronic transmission increases with the increasing diameter of the NTs, as the diameter increases with the increasing values of n ($3 \leq n \leq 7$). The slight diminishing effect in transmission has been observed due to the back scattering effect, which can be illustrated in Eq. (3).

$$T(E) \approx \frac{1-r}{1+r} \quad (3)$$

In Eq. (3), T(E), depends on backscattering coefficient r [21].

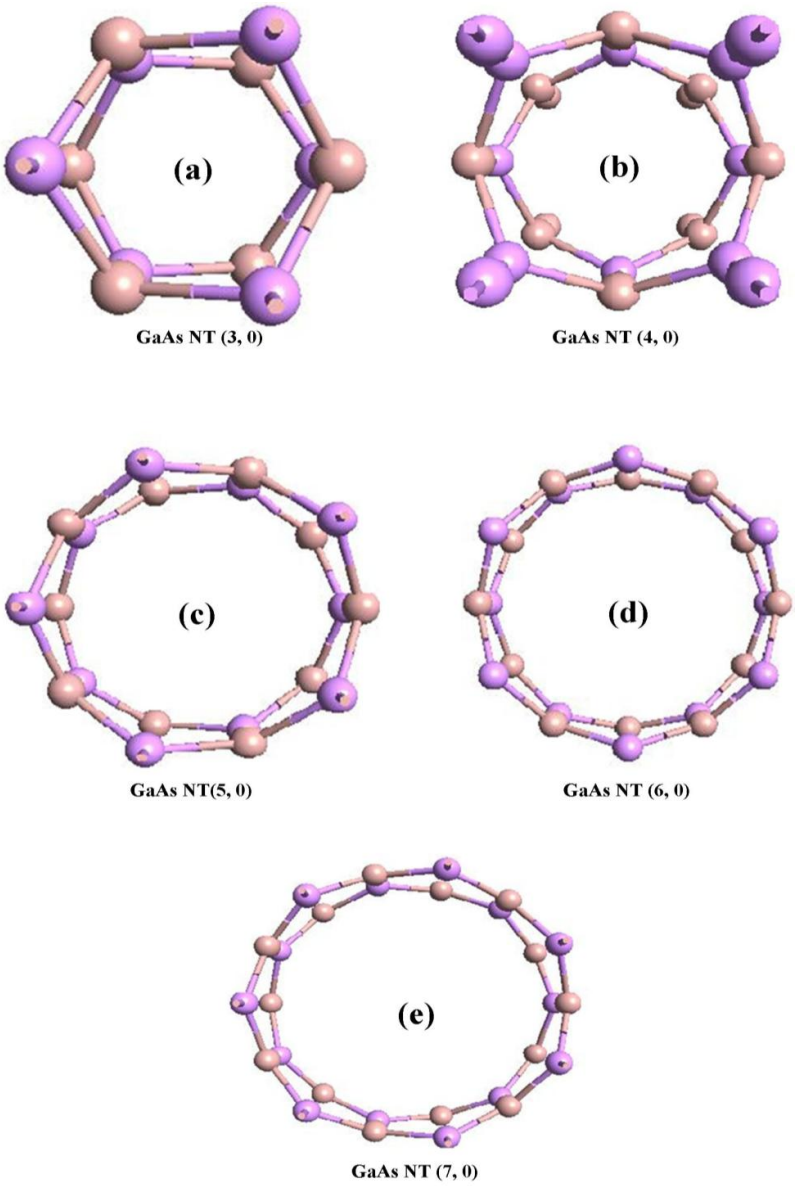

Fig.1: Initial and optimized geometry of GaAs SWNT's for different chiralities where $3 \leq n \leq 7$. (a): GaAs SWNT (3, 0) (b): GaAs SWNT (4, 0) (c): GaAs SWNT (5, 0) (d): GaAs SWNT (6, 0) (e): GaAs SWNT (7, 0).

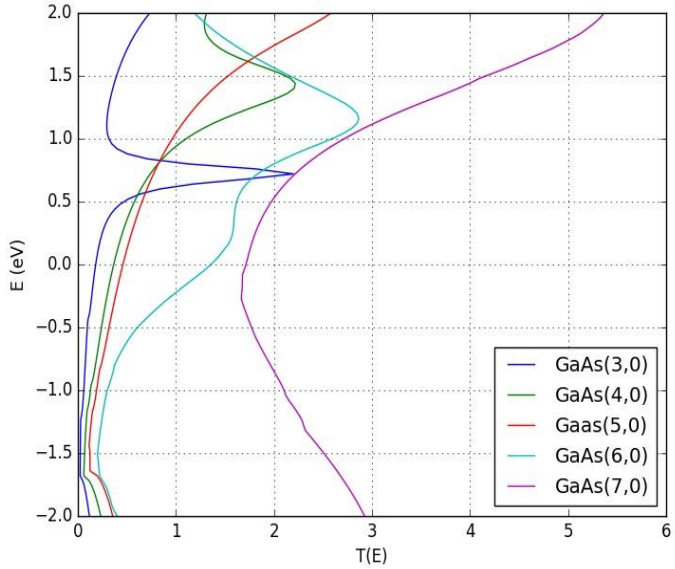

Fig. 2: Compared transmission spectra of GaAs SWNTs for different chiralities ($3 \leq n \leq 7$).

Device Density of States (DDOS), of the molecular device, means an energy level that electrons are allowed to occupy. DDOS gets affected by the broadening effect of the scattering region. DDOS can be formulated using the Lorentzian function in Eq. (4).

$$D(E) = \frac{\gamma/2\pi}{(E-\mu)^2+(\gamma/2)^2} \quad (4)$$

In Eq. (4), DDOS is represented as a function of available energy levels as D(E), γ is the broadening effect and μ is the chemical potential. The value of γ depends on the coupling strength of the electrodes with the central scattering region. Therefore γ is also related to coupling coefficient for atomic scale regime. In this case, the electrodes have been chosen as the extended parts of the central scattering region of the NTs. Thus strong coupling has been achieved during the operation.

The broadening effect received for (7, 0) NT is maximumly comparing with other NTs. Henceforth maximum broadens peaks are available for (7, 0) NT. This phenomenon reflects that higher the chiralities, higher is DDOS. This illustration satisfies that increasing diameter of NT increases DDOS. Enhanced DDOS is responsible for the high electronic transmission. Therefore channel conductivity increases accordingly. This reflects that high conducting current is available for higher chiralities NTs. The comparative image of band structures and DDOS for five different chiralities are shown in Fig.3(a), (b), (c), and 3(d), respectively. From this figure, it can be viewed that the bandgap increases with the increasing chiralities.

The binding energy (E_b) of the NTs, increase with increasing number of atoms, which is shown in Fig. 4. For (4, 0), (5, 0) and (6, 0) NTs, this energy is nearly equal. But for (7, 0) NT, this value suddenly rises to a great extent. This implies that binding energy increases with the increasing diameters of the NTs. This illustrates that the stability factor increases for higher chiralities NTs.

The NT devices are geometrically optimized with single ξ polarization. The total energy obtained for higher chiral vectors NTs is higher compared to lower chiralities. This energy has been divided for electrostatic and kinetic energy. The negative sign signifies the direction of applied bias voltages, as these energies, the external electric field. The changes in total energy with respect to chiral vector are shown in Fig. 5.

Highest Occupied Molecular Orbital (HOMO) and Lowest Unoccupied Molecular Orbital (LUMO) plot is an important feature of atomic scale analytical design. HOMO is the minima of the valence band and LUMO is the maxima of the conduction band. These two parameters have immense important during the consideration of the analytical design of nanoscale devices. The gap between HOMO and LUMO signifies the thermodynamic stability of the molecular device. Higher the gap higher is the stability.

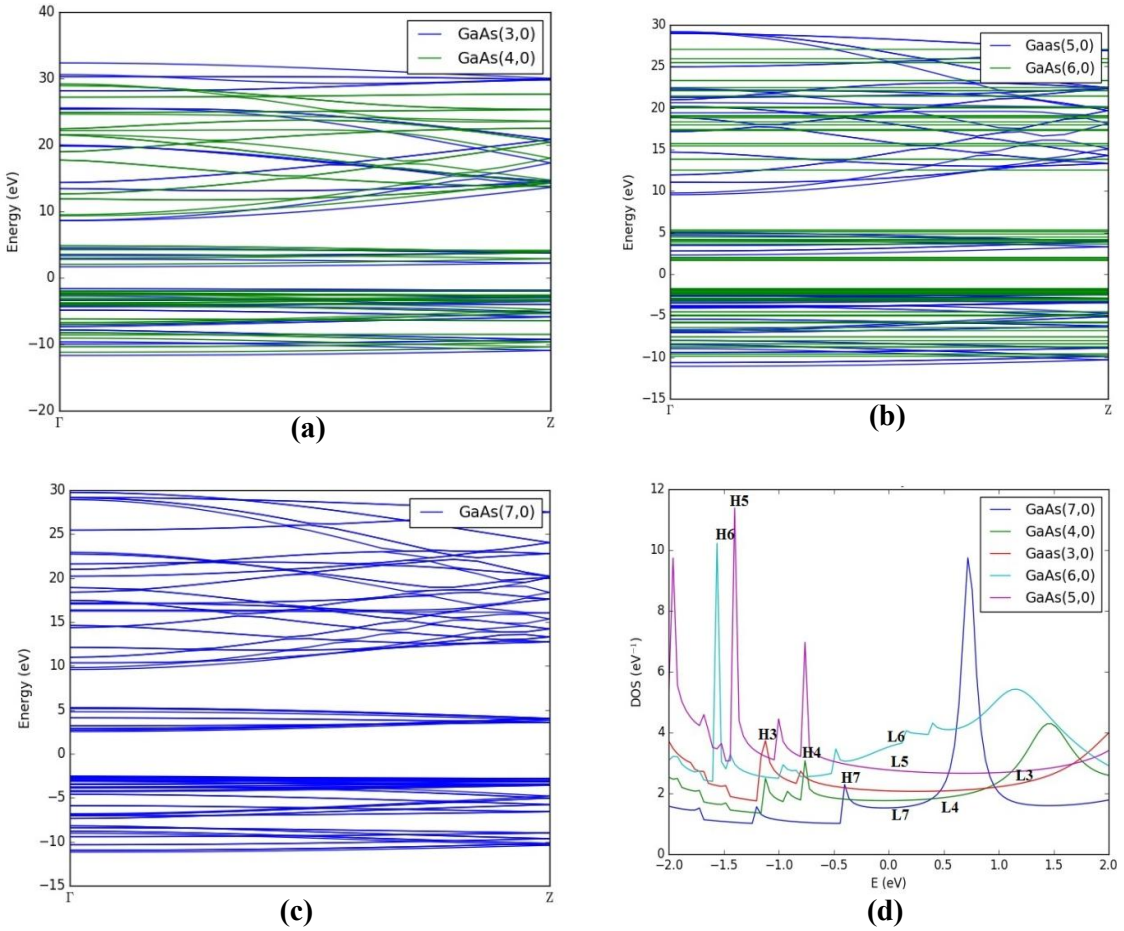

Fig. 3 (a) Compared bandstructure of (3, 0) and (4, 0) GaAs NT's, (b), Compared bandstructure of (5, 0) and (6, 0) GaAs NT's (c) Compared bandstructure of (7, 0) GaAs NT (d) compared DDOS of the GaAs NTs with n=3, 4, 5, 6 and 7.

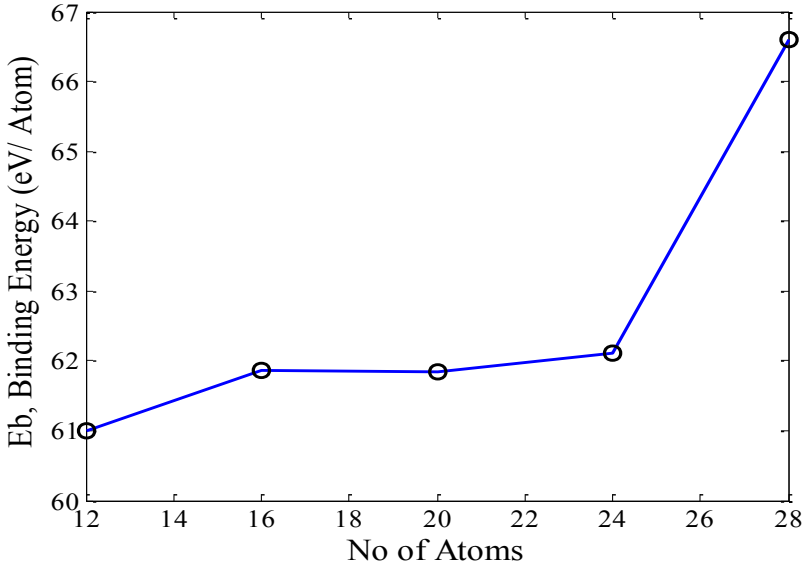

Fig. 4. Binding energy of the atoms varies with the number of atoms present in the NTs.

Due to the degeneracy of the highest populated molecular orbital, the maximum gap in HOMO-LUMO has been achieved, which is known as Jahn-Teller effect [21, 31]. The HOMO and LUMO obtained for different NT's already shown in Fig. 3(d). There is another explanation is associated with the gap between HOMO and LUMO. If the gap is higher than the potential barrier, thus the conductivity of the scattering region decreases. So the conducting current through the high barrier is lower. Table 3 shows the gap observed between HOMO and LUMO for the GaAs NTs. This table shows the charge transport capability and thermodynamic stability of the NT's in accordance with HOMO-LUMO. Buckling is the analytical instability which leads to failure of a device. Buckling occurs due to the compressive stress which is applied during the formation of NTs. The atomic force and stress have been kept minimal i.e.0.001eV/Å and 0.01eV/Å^3 respectively for the theoretical designing purpose of this model. The buckling has been reduced when the chiralities increase for the NTs. It implies the stability will be increased for higher chiralities NTs. This can be well depicted in Fig. 6. Therefore it can be illustrated that the stability of NTs will increase with the increasing chiral vector 'n' values. So purposely it is an important phenomenon that is observed during the theoretical modeling of GaAs NTs is that increasing diameter of NTs does not deteriorate its stability, whereas the stability factor gets increased with the higher values of the diameter of NTs.

It can be viewed from the Fig. 7, that the tendency of buckling occurs due to the electronegativity difference between Ga and As. Therefore the hybridization of these two atoms also varies. This degree of buckling decreases with the increase in the radius of NTs. Therefore from the plot in Fig. 6, it can be seen that the highest buckling is achieved for (3, 0) and lowest buckling is achieved for (7, 0).

The diameter, binding energy and total energy of the different NTs are shown in Table 4. The Current-Voltage (I-V) characteristics of the atomic scale device can be formulated using DFT and

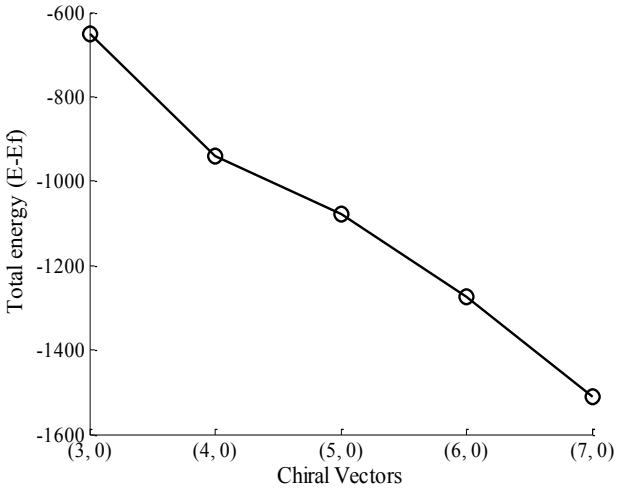

Fig. 5: Total energy of the NTs varies with the chiral vectors of the NTs.

Table 3: HOMO-LUMO obtained for the GaAs NTs with different chiral vectors.

GaAs NTs	(3, 0)	(4, 0)	(5, 0)	(6, 0)	(7, 0)
HOMO(eV)	-1.21	-0.74	-1.34	-1.4	-0.39
LUMO (eV)	1.3	0.52	0.19	0.11	0.01
$Gap_{HOMO-LUMO}$ (eV)	2.51	1.26	1.53	1.51	0.40
Charge transport capability	Moderate	Moderate	High	High	High
Thermodynamic stability	High	High	High	Moderate	Moderate

NEGF based first principle formalisms. The current flows between the two electrodes, within the scattering channel, is due to the potential drop arises near the central region of the NT, due to the potential difference occurs between the electrodes. Though the potential difference has been kept same for the different chiralities still the variation in current has been observed. Thus it can be illustrated as the diameter of the NT increases so that the respective channel conductivity and quantum-ballistic transmission increases for those NTs. The current can be formulated as in Eq. (5).

$$I = \frac{2q}{\hbar}\int T(E)M(E)(f_1 - f_2)dE \quad (5)$$

In Eq. (5), q is the columbic charge; $\hbar$ is the Plank's constant. Therefore it can be seen that I depends on transportation ability of the channel T(E), the number of independent channels M(E) and f_1 and f_2 are Fermi energy levels of the two electrodes respectively. M(E) also depends on the coupling coefficient and DDOS D(E) of the device, which is shown in Eq. (6). Henceforth, values of the transmission coefficient and DDOS of the NTs are increasing [21, 32]. The comparative graphs for different chiralities are shown in Fig. 7.

$$M(E) = \gamma D(E) \quad (6)$$

Finally, the cross-tick Table 5 shows the novelty of the proposed GaAs NTs comparing with existing NTs. The As atoms are more electronegative comparing with Ga atoms. Thus the degree of stability of this GaAs NT slightly hampered due to the unequal hybridization of the Ga and As atoms.

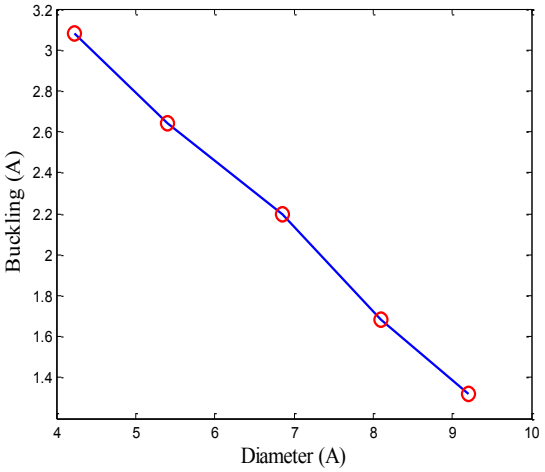

Fig. 6: Degree of buckling varies with the diameter of the NTs.

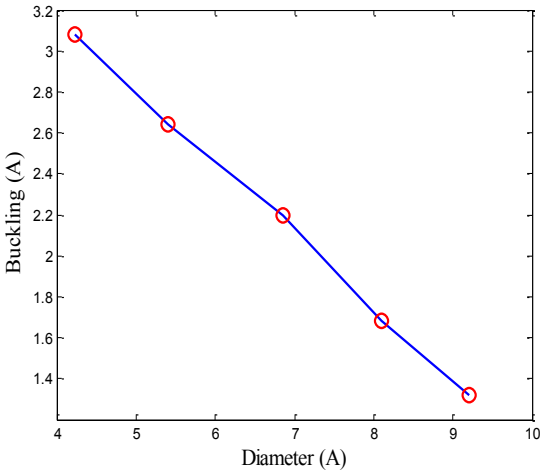

Fig. 7: Comparative study of I-V characteristics for various chiralities of NTs.

Table 4: Diameter, binding energy and total energy of the GaAs NTs for chirilities $3 \leq n \leq 7$.

Chirality(n,m)	No.of atoms	Bond length (Å)	Diameter (Å)	Binding energy (eV)	Total energy (eV)
(3,0)	12	2.43277	4.23	60.99	-650.71880
(4,0)	16	2.42725	5.40	61.86	-939.35371
(5,0)	20	2.41813	6.86	61.84	-1078.95137
(6,0)	24	2.40144	8.10	62.12	-1274.33561
(7,0)	28	2.36585	9.21	66.6	-1511.16139

Table 5: Cross-tick table for comparison of GaAs NTs with various others NTs.

Features \ ExistingNTs	GaP NT [7]	SnCNT [8]	AuNT [14]	C-B heterjunction NT [33]	Lightly Doped CNTFET[34]	Light driven doped TiO_2 [35]	Proposed GaAs NT
Extremly small applied bias voltage (V)	√	√	×	√	√	×	√
Ultra low diameter of NT (nm)	√	√	√	√	√	×	√
Ultra high operating frequency	×	√	√	×	×	×	√
Minimal stress tolerance	×	×	×	×	×	×	√
Minimal force tolerance	√	×	√	×	×	×	√
Presence of optical property	×	×	×	×	×	√	√
Presence of variation in chiral vector	√	√	√	×	×	×	√
High conducting current	√	√	×	√	√	×	√
Possibility of room temperature operation	×	√	×	×	×	×	√
Electrical doping applied	×	×	×	×	×	×	√

CONCLUSION

The electronic transport property and the structural stability of GaAs NTs ($3 \leq n \leq 7$) have been investigated and discussed using ATK-VNL software Quantumwise simulator version 13.8.0. It has been observed that the stability of the NTs increases with the increasing diameter of the NTs. By introducing electrical doping procedure we have enhanced the device performance. As a result, high current flows through the central molecular region of the device. The peaks observed in the DDOS of the NTs more broaden when increasing the diameter of the tubes. Similarly, the electronic transmission, scattering channel conductivity, and current through the scattering region increase with the increasing diameter and chiralities of the NTs. These NTs have operated at room temperature with ultra-high frequency *i.e.* 1000THz. The buckling of the tubes minimized when the diameter of the NTs increase. This proves that theses NTs are structurally stable if the tube diameters increase rapidly. The Slight buckling effect arises for this NT, due to the difference in hybridization of Gallium and Arsenic atoms. This does not happen for conventional CNT.

ACKNOWLEDGEMENT

Authors are grateful to University Grants Commission (UGC) for sanctioning a research project having File no.: 41-631/2012(SR) and Quantumwise A/S version 13.8.0 under which this paper has been completed.

CONFLICT OF INTEREST

The authors declare that there is no conflict of interests regarding the publication of this manuscript.

REFERENCES

[1] Ghorbani-Asl M., Paul D., Koziol B., Koziol K., (2015), A computational study of the quantum transport properties of a Cu-CNT composite. *Phy. Chem. Chem. Phy.* 17: 18273-18277.

[2] Choudhary S., Varshney M., (2015), First-principles study of spin transport in CrO_2-CNT-CrO_2 magnetic tunnel junction. *J. Superconduc. Novel Magnetism*. 28: 3141-3145.

[3] Choudhary S., Jalu S., (2015), First-principles study of spin transport in Fe-SiCNT-Fe magnetic tunnel junction. *Phys.*

Lett. A. 379: 1661-1665.
[4] Jain N., Manhas S., Aggarwal A. K., Chaudhry P. K., (2014), Effect of metal contact on CNT based sensing of NO_2 molecules. *In Phys. Semiconduc. Devices*. (pp. 637-639). Springer.
[5] Kolchuzhin V., Mehner J., Markert E., Heinkel U., Wagner C., Schuster J., Gessner T., (2014), System-level-model development of an SWCNT based piezoresistive sensor in VHDL-AMS. In Thermal, mechanical and multi-physics simulation and experiments in microelectronics and microsystems (eurosime). *2014 15th Int. Conf.* (pp. 1-6). IEEE.
[6] Husain M. M., (2013), Carbon dioxide adsorption on single walled bamboo-like carbon nanotubes (SWBCNT): A computational study. *Int. J. Res. Eng. Sci. (IJRES).* 1: 13-26.
[7] Srivastava A., Jain S. K., Khare P. S., (2014), Ab-initio study of structural, electronic, and transport properties of zigzag GaP nanotubes. *J. Molec. Model.* 20: 2171-2177.
[8] Samanta P. N., Das K. K., (2014), Electron transport properties of zigzag single walled tin carbide nanotubes. *Comput. Mater. Sci.* 81: 326-331.
[9] Yamacli S., (2014), Investigation of the voltage-dependent transport properties of metallic silicon nanotubes (SiNTs): A first-principles study. *Comput. Mater. Sci.* 91: 6-10.
[10] Guo Y. D., Yan X. H., Xiao Y., (2014), The spin-dependent transport of Co-encapsulated Si nanotubes contacted with Cu electrodes. *Appl. Phys. Lett.* 104: 063103-063108.
[11] Choudhary S., Qureshi S., (2012), Effect of moisture on electron transport in Si C nanotubes: An ab-initio study. *Phys. Lett. A.* 376: 3359-3362.
[12] Li E., Hou L., Cui Z., Zhao D., Liu M., Wang X., (2012), Electronic structures and transport properties of single crystalline gan nanotubes. *Nano*. 7: 1250014-1250019.
[13] Li E., Cui Z., Liu M., Wang X., (2012), First-principles study on transport properties of saturated single crystalline GaN nanotubes. *Integrat. Ferroelect.* 137: 134-142.
[14] Cai Y., Zhou M., Zeng M., Zhang C., Feng Y. P., (2011), Adsorbate and defect effects on electronic and transport properties of gold nanotubes. *Nanotechnol*. 22: 215702-215707.
[15] Gao W., Kahn A., (2003), Electrical doping: The impact on interfaces of π-conjugated molecular films. *J. Phys.: Condensed Matter.* 15: S2757-S2762.
[16] Rudaz S. L., (1998), U.S. Patent No. 5,729,029. Washington, DC: U.S. Patent and Trademark Office.
[17] Yu S., Frisch J., Opitz A., Cohen E., Bendikov M., Koch N., Salzmann I., (2015), Effect of molecular electrical doping on polyfuran based photovoltaic cells. *Appl. Phys. Lett.* 106: 54-61.
[18] Kahn A., Koch N., Gao W., (2003), Electronic structure and electrical properties of interfaces between metals and π-conjugated molecular films. *J. Polym. Sci. Part B.: Polym. Phys.* 41: 2529-2548.
[19] Dey D., Roy P., Purkayastha T., De D., (2016), A first principle approach to design gated pin nanodiode. *J. Nano Res. Trans. Tech. Publications*. 36: 16-30.
[20] Dey D., Roy P., De D., (2015), Molecular modeling of nano bio pin FET. In VLSI Design and Test (VDAT), 2015 19th. *Int. Symp. IEEE*. 1-6.
[21] Dey D., Roy P., De D., (2016), Electronic characterisation of atomistic modelling based electrically doped nano bio pin FET. *IET Computers & Digital Techniq.* 10: 273-285.
[22] Han Q., Cao B., Zhou L., Zhang G., Liu Z., (2011), Electrical transport study of single-walled ZnO nanotubes: A first-principles study of the length dependence. *J. Phys. Chem. C*. 115: 3447-3452.
[23] Kohn W., Sham L. J., (1965), Self-consistent equations including exchange and correlation effects. *Phys. Rev.* 140: A1133-A1138.
[24] Gross E. K., Dreizler R. M., (Eds.), (2013), *Density functional theory* (Vol. 337). Springer Science & Business Media.
[25] Atomistix ToolKit version 13.8.0, QuantumWise A/S (www quantumwise.com).
[26] Zienert A., Schuster J., Streiter R., Gessner T., (2010), Transport in carbon nanotubes: Contact models and size effects. *Phys. Status Solid. (b).* 247: 3002-3005.
[27] Renugopalakrishnan V., Madrid G., Cuevas G., Hagler A. T., (2000), Density functional studies of molecular structures of N-methyl formamide, N, N-dimethyl formamide, and N, N-dimethyl acetamide. *J. Chem. Sci.* 112: 35-42.
[28] Chauhan S. S., Srivastava P., Shrivastava A. K., (2014), Electronic and transport properties of boron and nitrogen doped graphene nanoribbons: An ab initio approach. *Appl. Nanosci.* 4: 461-467.
[29] Stokbro K., (2008), First-principles modeling of electron transport. *J. Phys.: Cond. Mat.* 20: 064216-064221.
[30] Datta S., (2005), Quantum transport: Atom to transistor. *Cambridge University Press.*
[31] Mealli C., (2006), Computational inorganic chemistry, in Bartini, I. (Ed.): 'Encyclopedia of life support systems (EOLSS)' (Developed under the Auspices of the UNESCO, *Eolss Publishers Oxford*, UK, 1-45.
[32] Xia C. J., Liu D. S., Liu H. C., (2012), Phenylazoimidazole as a possible optical molecular switch: An ab initio study. *Optik-Int. J. Light and Electron Optics*. 123: 1307-1310.
[33] Jiuxu S., Yintang Y., Hongxia L., Lixin G., (2011), Negative differential resistance in an (8, 0) carbon/boron nitride nanotube heterojunction. *J. Semiconduc.* 32: 042003-042009.
[34] Sedigh Ziabari S. A., Tavakoli Saravani M. J., (2017), A novel lightly doped drain and source Carbon nanotube field effect transistor (CNTFET) with negative differential resistance. *Int. J. Nano Dimens.* 8: 107-113.
[35] Zakeri S. M. E., Asghari M., Feilizadeh M., Vosoughi M., (2014), A visible light driven doped TiO_2 nanophotocatalyst: Preparation and characterization. *Int. J. Nano Dimens.* 5: 329-335.